Biochemical and Biophysical Research Communications 452 (2014) 801–807

Contents lists available at ScienceDirect

Biochemical and Biophysical Research Communications

journal homepage: www.elsevier.com/locate/ybbrc

Activation of RAS/ERK alone is insufficient to inhibit RXRα function and deplete retinoic acid in hepatocytes

Ai-Guo Wang *, Ya-Nan Song, Jun Chen, Hui-Ling Li, Jian-Yi Dong, Hai-Peng Cui, Liang Yao, Xue-Feng Li, Wen-Ting Gao, Ze-Wen Qiu, Fu-Jin Wang, Jing-Yu Wang *

Laboratory Animal Center, Dalian Medical University, Dalian, Liaoning 116044, PR China

ARTICLE INFO

Article history:
Received 19 August 2014
Available online 12 September 2014

Keywords:
H-*ras*12V
Hepatic tumor
RXRα
Retinoic acid

ABSTRACT

Activation of RAS/ERK signaling pathway, depletion of retinoid, and phosphorylation of retinoid X receptor alpha (RXRα) are frequent events found in liver tumors and thought to play important roles in hepatic tumorigenesis. However, the relationships among them still remained to be elucidated. By exploring the transgenic mouse model of hepatic tumorigenesis induced by liver-specific expression of H-*ras*12V oncogene, the activation of RAS/ERK, the mRNA expression levels of retinoid metabolism-related genes, the contents of retinoid metabolites, and phosphorylation of RXRα were determined. RAS/ERK signaling pathway was gradually and significantly activated in hepatic tumor adjacent normal liver tissues (P) and hepatic tumor tissues (T) of H-*ras*12V transgenic mice compared with normal liver tissues (Wt) of wild type mice. On the contrary, the mRNA expression levels of retinoid metabolism-related genes were significantly reduced in P and T compared with Wt. Interestingly, the retinoid metabolites 9-*cis*-retinoic acid (9cRA) and all-*trans*-retinoic acid (atRA), the well known ligands for nuclear transcription factor RXR and retinoic acid receptor (RAR), were significantly decreased only in T compared with Wt and P, although the oxidized polar metabolite of atRA, 4-keto-all-*trans*-retinoic-acid (4-keto-RA) was significantly decreased in both P and T compared with Wt. To our surprise, the functions of RXRα were significantly blocked only in T compared with Wt and P. Namely, the total protein levels of RXRα were significantly reduced and the phosphorylation levels of RXRα were significantly increased only in T compared with Wt and P. Treatment of H-*ras*12V transgenic mice at 5-week-old or 5-month-old with atRA had no effect on the prevention of tumorigenesis or cure of developed nodules in liver. These events imply that the depletion of 9cRA and atRA and the inhibition of RXRα function in hepatic tumors involve more complex mechanisms besides the activation of RAS/ERK pathway.

1. Introduction

Hepatocellular carcinoma (HCC) is the seventh most common cancer and the third leading cause of cancer related mortality worldwide [1]. Annually, more than 620,000 new patients are diagnosed with this disease and one-year survival rates remain less than 50% [2]. The main risk factors such as viral hepatitis, alcohol abuse, aflatoxin, metabolic disorders (e.g., long-lasting diabetes mellitus), and fatty liver contribute to increasing incidence rates of HCC [3–6]. Independent of the above risk factors, numerous researches showed that the hyperactivation of Ras-dependent signal transduction pathway is a frequent event in human hepatocarcinogenesis and the inhibitor of Ras-mediated signaling pathway has been proved to be an efficient treatment for HCC patients [7,8]. Also, the depletion of retinoid has been frequently found in HCC [9] and epidemiological and experimental reports showed that application of retinoid atRA can prevent liver cancer [10]. In addition, phosphorylation of RXRα is also a frequently observed event in HCC [11] and the acyclic retinoid (ACR), a synthetic retinoid which is believed to recover the RXRα function, exerts chemopreventive effects in HCC patients [12]. However, relationships among the activation of Ras-mediated signaling pathway, depletion of hepatic retinoid, and phosphorylation of RXRα still remained to be elucidated.

It has been suggested that the activation of RAS/ERK pathway could repress the expression of retinoid metabolism-related cytochrome P450 (CYP) genes [13,14] and phosphorylate RXRα [11,12]. However, these findings were few verified in spontaneously developed hepatic tumors induced by *ras* oncogene *in vivo*. Animal models are useful tools for understanding the

* Corresponding authors. Fax: +86 411 86110171.
E-mail addresses: wangaiguotl@hotmail.com (A.-G. Wang), wangjingyus@163.com (J.-Y. Wang).

http://dx.doi.org/10.1016/j.bbrc.2014.09.007
0006-291X/

underlying molecular mechanisms in the process of hepatocarcinogenesis, especially for the early stages [15]. We have established transgenic mice lineages expressing H-*ras*12V oncogene special in hepatocytes and developing liver tumors with high reproducibility at the appropriate time [16]. In this study, by exploring this hepatic tumorigenesis model, we found that the activation of the RAS/ERK pathway alone in hepatic tumor adjacent normal liver tissues of transgenic mice was not efficient to induce the depletion of retinoid and the inhibition of RXRα function. But these events did happen in hepatic tumor tissues of transgenic mice. Therefore, additional molecular changes must be involved besides the activation of RAS/ERK pathway. Moreover, due to the depletion of retinoid and inhibition of RXRα function happened only in hepatic tumors, the contribution of them to oncogene *ras*-induced hepatic tumorigenesis remains to be further elucidated.

2. Materials and methods

2.1. Experimental animals and histopathological examination

Procedures for animal handling and tissue sampling were conducted in compliance with protocols approved by the Animal Care and Use Committee of Dalian Medical University. C57BL/6J wild type mice and H-*ras*12V transgenic mice were breeding and housed in Laboratory Animal Center of Dalian Medical University. Eight-month-old males were killed and parts of wild type normal liver tissues (Wt), hepatic tumor adjacent normal liver tissues (P) and hepatic tumor tissues (T) of H-*ras*12V transgenic mice were removed and immediately flash-frozen in liquid nitrogen. The remaining tissue parts were fixed in 10% neutral buffered formalin, embedded in paraffin, sectioned, and stained with hematoxylin and eosin using standard methods, and then underwent histopathological examination. The morphological diagnosis confirmed Wt, P and T tissues were used for the subsequent experimental procedures.

2.2. Different gene expression by next generation sequencing (NGS) analysis

Tissues from five wild type mice and five H-*ras*12V transgenic mice were chosen for total RNA extraction by TRIzol reagent (Invitrogen, Grand Island, NY). Total RNA quantity and concentration was analyzed on a ND-8000 spectrophotometer (Nanodrop, Technologies, Wilmington, DE).

Due to the consistent inbred genetic background, the definite etiology (*ras* oncogene) for hepatic tumor development and the consistent pathological features of the samples in each group, the total RNA samples from the same group were mixed equivalently to generate three composite samples, i.e., Wt, P and T. Preparation of the mRNA sample for RNA-Seq analysis was performed using the TruSeq® RNA LT Sample Prep Kit v2 (Illumina, San Diego, CA). The template molecules were used for cluster generation and sequencing on the Illumina HiSeq 2000 (Illumina, San Diego, CA) instrument. One sample per lane was used to generate 50 bp single end reads. Read alignment was performed by using Tophat v1.3.2 to the UCSC Mouse reference genome (mm10, http://genome.ucsc.edu/). Transcript assembly and quantification were performed by Cufflinks v2.0.2 to process the Tophat alignments. The assembled Cufflinks transcripts were processed with the Cuffcompare analytical strategies to detect differentially expressed genes. The database for annotation, visualization, and integrated discovery (DAVID) v6.7 was used to interpret the differentially expressed gene pools.

2.3. RT-qPCR

Total RNA was isolated from another sample sets from Wt, P, and T using the TRIzol reagent (Tiangen, Beijing, CHN). According to manufacturer's instructions, 3 μg of total RNA were reverse transcribed to single-stranded cDNA using a reverse transcription system (Tiangen, Beijing, CHN) and then performed qPCR experiments using SYBR Green (Real Master Mix (SYBR Green), Tiangen) on Applied Biosystems StepOnePlus Real-Time PCR System. The primers used to detect the expression of target genes were showed in Table S1. A separate RT-qPCR using primer for the detection of 18s was used as a control.

2.4. Determination of retinoid metabolites in liver samples by LC–MS/MS

A 50 mg tissue sample was homogenized in 300 μL distilled water and then extracted with 1.2 mL ethylacetate. The upper organic layer was collected and evaporated to dryness at 40 °C under a gentle stream of nitrogen gas. The residue was dissolved in 200 μL mobile phase. A 10 μL aliquot was injected into the LC–MS/MS instrument (API 3200; Applied Biosystems, Foster City, CA, USA) for analysis. Quantification was done using the multiple reaction monitoring (MRM) transition m/z = 299/255 for atRA and 9cRA, m/z = 313/269 for 4-KETO-at-RA, and m/z = 283/283 for at-RAL and 9-*cis*-RAL. The declustering potential (DP) was set at 35 eV, 25 eV and 38 eV and the entrance potential (EP) was set at 22 eV, 20 eV and 22 eV, respectively.

The chromatograph was equipped with a Cap Cell Pack C_{18} (150 × 2.1 mm i.d., 3.5 μm) analytical column. The mobile phase was consisted of methanol-0.5% ammonium acetate aqueous solution for a gradient elution at 0–3 min (20:80, v/v), 3–20 min (20 → 100:80 → 0, v/v), and 22–30 min (20:80, v/v) at a flow rate of 0.5 mL/min.

2.5. Western blotting

Tissue lysates were prepared by homogenizing flash-frozen tissues in lysis buffer. For Western blot analysis, equal amounts (30 mg) of proteins were resolved by SDS–PAGE and transferred to a polyvinylidene difluoride membrane (Millipore, Billerica, MA). The membranes were probed with the primary and secondary antibodies: anti-RXRα (ΔN 197) SC-774 and horseradish peroxidase (HRP)-conjugated goat anti-rabbit IgG antibodies (Santa Cruz Biotechnology, Santa Cruz, CA); anti-phospho-p44/42 Map Kinase (Thr202/Tyr204) and anti-44/42 Map Kinase antibodies (Cell Signaling, Frankfurt, Germany); anti-RXRα polyclonal antibody (21218-1-AP) (Proteintech Group, USA); anti-GAPDH (Trevigen, Gaithersburg, MD); and HRP-conjugated goat anti-mouse IgG (Amersham Biosciences, Buckinghamshire, UK). Positive bands were detected using the Enhanced Chemiluminescence system (BeyoECL Plus) (Beyotime Institute of Biotechnology, CHN).

2.6. Treatment of mouse with all-trans retinoic acid (atRA)

Thirty H-*ras*12V transgenic mice, randomly divided into two groups, were treated with feeding atRA (8.33 mg/kg/day). The treatment of one group started at 5-week-old and another at 5-month-old. Ten H-*ras*12V transgenic mice without treatment were used as control group. At 8-month-old, the mice were sampled and the data related to the liver/body weight and pathological changes, number and size of tumor were collected and analyzed.

2.7. Statistical analysis

Data were presented as means ± S.D. Differences in means were analyzed by Student's *t* test. Pathological change incidence (%) was analyzed by chi-square analysis. *P* values <0.05 were considered significant.

3. Results

3.1. H-ras12V transgenic mice developed liver tumors at 8-month-old

We classified the hepatic tumors as hepatic adenoma (HCA) and hepatocellular carcinoma (HCC) according to the modified methods of Frith and Ward [16]. For H-*ras*12V transgenic mice, gross findings for hepatic tumors were a yellowish-brown color, and were of various sizes with single or multiple nodules in the liver (Fig. S1B). Microscopic HCA lesions were relatively well-circumscribed and the hepatocytes around the tumor lesions were compressed (Fig. S1D). The HCC was: (1) large in size, and typically more than 5 mm in diameter; (2) showed a trabecular arrangement of tumor cells; and (3) contained highly anaplastic cells with evidence of necrosis (data not shown). All HCA (Fig. S1D) and HCC showed abundant fatty deposits. No signs of cirrhosis, inflammation, and necrosis were detected. For liver tissues of wild type mice and hepatic tumor adjacent normal liver tissues of H-*ras*12V transgenic mice, no histopathological changes were detected (Fig. S1). We performed the following experiments based on the samples from liver tissues of wild type mice (Wt), hepatic tumor adjacent normal liver tissues (P) and HCA tissues (T) of transgenic mice. The HCA tissues were selected because they were in the early stage of tumorigenesis and represented the majority type of hepatic tumors developed in H-*ras*12V transgenic mice at 8-month-old.

3.2. The mRNA expression levels of genes related to retinoid metabolism were significantly reduced in H-ras12V transgenic mice

In order to investigate if the mRNA expression levels of retinoid metabolism-related genes were regulated in H-*ras*12V induced tumors, the Next Generation Sequencing (NGS) analysis was performed to screen the mRNA expression profile and the DAVID v6.7 software was used to analyze the enrichment of GO terms. To our surprise, the retinoid metabolism was rated to the top three significantly changed pathways among Wt, P and T in pair-wise comparison (Fig. S2). And the significantly changed genes were mainly related to the metabolism from 9-*cis*-retinal (9cRAL) and all-*trans*-retinal (atRAL) to 9-*cis*-retinoic acid (9cRA) and all-*trans*-retinoic acid (atRA), respectively, and from atRA to oxidized polar metabolites such as 18-hydroxy-retinoic acid, 4-Keto-retinoic acid (4-Keto-RA), and retinoyl β-glucuronide (Fig. S3). To confirm the data from the NGS analysis, eight genes were selected for further analysis by RT-qPCR. Consistent to the NGS data, the examined retinoid metabolism-related genes were significantly reduced in the P and T tissues compared with Wt (Fig. 1, Table S2). Interestingly, the majority of the significantly changed cytochrome P450 (CYP) genes, including the retinoid metabolism-related CYP genes, were significantly down-regulated in both P and T compared to Wt along with RAS/ERK activation by NGS analysis (Table 1, Table S3).

3.3. Retinoid metabolites were significantly reduced in tumor tissues of H-ras12V transgenic mice

To find out if the down-regulated expression of retinoid metabolism-related genes resulted in the decreased contents of retinoid metabolites, LC–MS/MS was used to detect the concentrations of retinoid metabolites in the samples. As expected, there was no significant difference for 9cRAL contents among Wt, P, and T tissues (Fig. 2A). Interestingly, although there was no significant difference between Wt and P for the contents of atRA and 9cRA, both of them were significantly reduced in T tissues compared to the Wt and P (Fig. 2B and C). The content of 4-Keto-RA was significantly reduced in both P and T compared to Wt tissues (Fig. 2D). In addition, no difference was detected among Wt, P, and T tissues for the content of atRAL (data not shown).

3.4. RXRα was only significantly phosphorylated in tumor tissues of H-ras12V transgenic mice

It has been reported that RAS/ERK pathway can phosphorylate the RXRα and disable its functions in human HCC [11]. To confirm this event in H-*ras*12V transgenic mice, the total protein and phosphorylation level of ERK, and the mRNA, total protein and phosphorylation level of RXRα were examined in Wt, P, and T samples. The level of p-ERK was elevated not only in T, but also in P tissues compared to Wt, even though the level of p-ERK in T tissues was much higher than P. Interestingly, the total protein level of ERK was elevated only in T tissues compared to Wt and P (Fig. 3A). Although there was no difference among Wt, P, and T tissues in the mRNA level of RXRα (Fig. 3B), the total protein level of RXRα was much reduced in T tissues compared to Wt and P. To our surprise, the level of p-RXRα was significantly elevated only in T tissues compared to Wt and P (Fig. 3A). These results indicate that additional mechanisms must be involved for the post-transcript regulation of RXRα and the phosphorylation of RXRα in T tissues besides the activation of RAS/ERK pathway.

3.5. No effect of atRA on preventing the liver tumorigenesis and curing the developed hepatic nodules induced by H-ras12Voncogene

It was reported epidemiologically and experimentally that atRA could prevent cancer in various organs including the stomach, breast, lung, prostate, and liver [10]. In H-*ras*12V transgenic mice, there is no histopathological change could be detected in liver tissues at 5-week-old. However, at 5-month-old, the mice develop multiple hepatic nodules [16]. To investigate if the atRA could prevent the tumorigenesis and cure the developed nodules induced by H-*ras*12V, the atRA was feed to 5-week-old and 5-month-old H-*ras*12V transgenic mice and, at 8-month-old, the mice were sampled. The results showed that no difference was detected for size, number (Fig. 4A and B), and histopathological change (data not shown) of hepatic tumors, and for the liver/body weight (Fig. 4C) between treated and untreated H-*ras*12V transgenic mice. These data indicate that atRA alone is not efficiency to prevent the tumorigenesis and cure the developed nodules induced by *ras* oncogene.

4. Discussion

In present study, no difference was detected for the protein levels of total RXRα or p-RXRα in P tissues compared to Wt, even though the RAS/ERK pathway was significantly activated in P. Curiously, the functions of RXRα were significantly blocked in T tissues. Namely, the total protein level of RXRα was significantly down-regulated and the phosphorylation level of RXRα was significantly up-regulated in T tissues compared with Wt and P (Fig. 3A). While, no significant difference was detected for the mRNA expression levels of RXRα among Wt, P, and T tissues (Fig. 3B). Taken together, these data indicate that activation of RAS/ERK pathway alone does not effectively inhibit RXRα function. Thus, additional mechanisms must be involved in post-transcription regulation and phosphorylation of RXRα in hepatic tumor cells besides RAS/ERK activation.

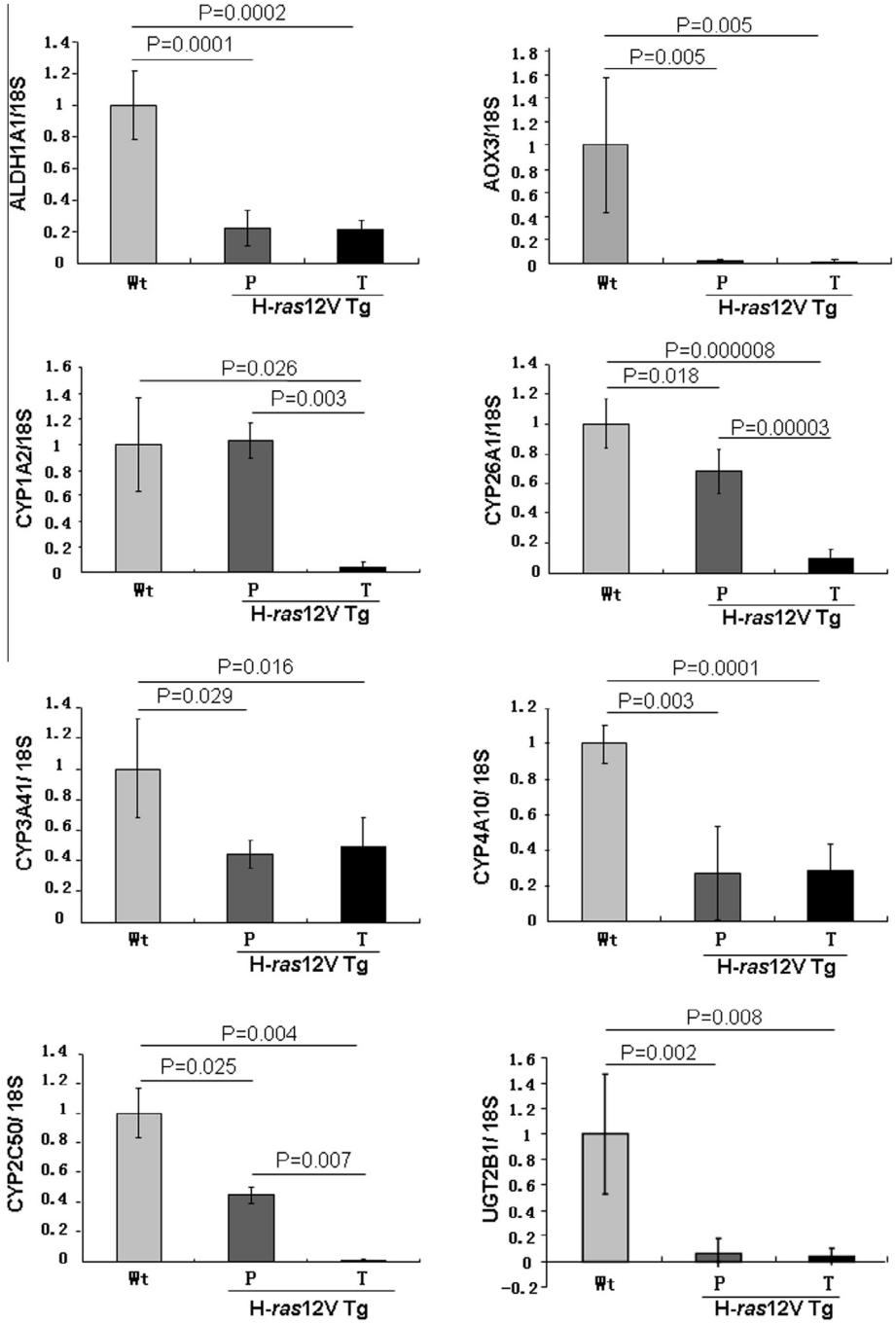

Fig. 1. The mRNA expression levels of retinoid metabolism-related genes confirmed by qRT-PCR. The mRNA expression levels of genes were normalized to 18s. Wt: wild type mice; P: hepatic tumor adjacent normal liver tissues; T: hepatic tumor tissue. Data are expressed as mean ± S.D. (n = 5).

Indeed, a recent *in vitro* study showed that PI3K may be involved in the phosphorylation of RXRα in human hepatoma cells [17].

Similarly, depletion of retinoic acid (RA) was also only found in T tissues (Fig. 2). The new evidence casts doubt on the important anti-tumorigenesis roles of RXRα and RA. While, the acyclic retinoid (ACR), a synthetic retinoid (a weak ligand to RXRα compared to RA), has exerted chemopreventive effects in HCC cells [12]. Recent evidence indicates that ACR has multiple antitumor functions beyond its role as RXRα agonist [11]. Collectively, we speculate that the dysfunction of RXRα and depletion of RA may be the by-product of hepatic tumorigenesis or favor the development of hepatic tumor.

The expression of major cytochrome P450 (CYP) genes is commonly repressed in the tumor tissues from patients suffering HCC and hepatocyte tumor cell lines compared to primary human hepatocytes [18,19]. The RAS/ERK signaling cascade is thought to contribute to repress the expression of CYP genes besides its functions of hepatocarcinogenesis and dedifferentiation in hepatocyte tumors [14,20]. Consistently, majority of significantly changed cytochrome P450 (CYP) genes were significantly down-regulated in both P and T compared to Wt along with the activation of RAS/ERK by NGS analysis (Tables 1 and S3). These data indicate that the activation of RAS/ERK pathway plays important roles in repressing the expression of CYP genes *in vivo*. Importantly, our

Table 1
Significantly down-regulated CYP genes in both P and T of H-ras12V transgenic mice compared to Wt detected by NGS analysis.

Genes	FPKM value			T vs W		P vs W		T vs P	
	Wt	P	T	*p* value	Up/down	*p* value	Up/down	*p* value	Up/down
Cyp2c50	3.51E+02	1.34E+02	5.48E+00	0.00E+00	Down	7.18E−03	Down	5.84E−14	Down
Cyp2c54	2.12E+02	1.08E+02	4.91E+00	0.00E+00	Down	4.01E−02	Down	1.99E−13	Down
Cyp8b1	6.44E+01	1.25E+01	1.31E+00	0.00E+00	Down	6.45E−09	Down	5.54E−07	Down
Cyp4a14	5.66E+01	3.57E+00	2.84E−01	0.00E+00	Down	0.00E+00	Down	3.96E−06	Down
Cyp26a1	2.17E+01	4.82E+00	5.17E−01	2.26E−12	Down	1.34E−06	Down	3.15E−05	Down
Cyp4a10	6.93E+01	1.74E+01	4.27E+00	3.48E−12	Down	1.02E−06	Down	2.90E−04	Down
Cyp3a41b	1.24E+02	2.54E+01	7.68E+00	4.88E−12	Down	4.49E−08	Down	1.02E−03	Down
Cyp3a41a	1.27E+02	2.72E+01	8.30E+00	1.61E−11	Down	1.56E−07	Down	1.05E−03	Down
Cyp2c38	1.52E+01	8.12E+00	6.27E−01	2.11E−11	Down	3.35E−02	Down	3.72E−08	Down
Cyp3a16	9.96E+01	3.30E+01	8.57E+00	5.10E−10	Down	1.31E−04	Down	2.41E−04	Down
Cyp3a44	7.94E+01	3.18E+01	1.04E+01	2.30E−07	Down	1.45E−03	Down	1.82E−03	Down
Cyp2c55	5.54E+00	1.20E+00	3.19E−01	2.54E−06	Down	1.90E−04	Down	2.86E−02	Down
Cyp2d22	3.13E+01	4.10E+00	2.44E+00	3.63E−10	Down	2.89E−12	Down	1.75E−01	–
Cyp4f14	1.26E+01	3.40E+00	7.24E−01	1.02E−08	Down	3.14E−03	Down	8.39E−01	–
Cyp4a32	2.38E+01	1.17E+01	6.42E+00	1.03E−03	Down	1.50E−02	Down	1.16E−01	–
Cyp2b10	4.27E+00	1.31E+00	1.35E+00	2.90E−02	Down	5.49E−03	Down	9.55E−01	–

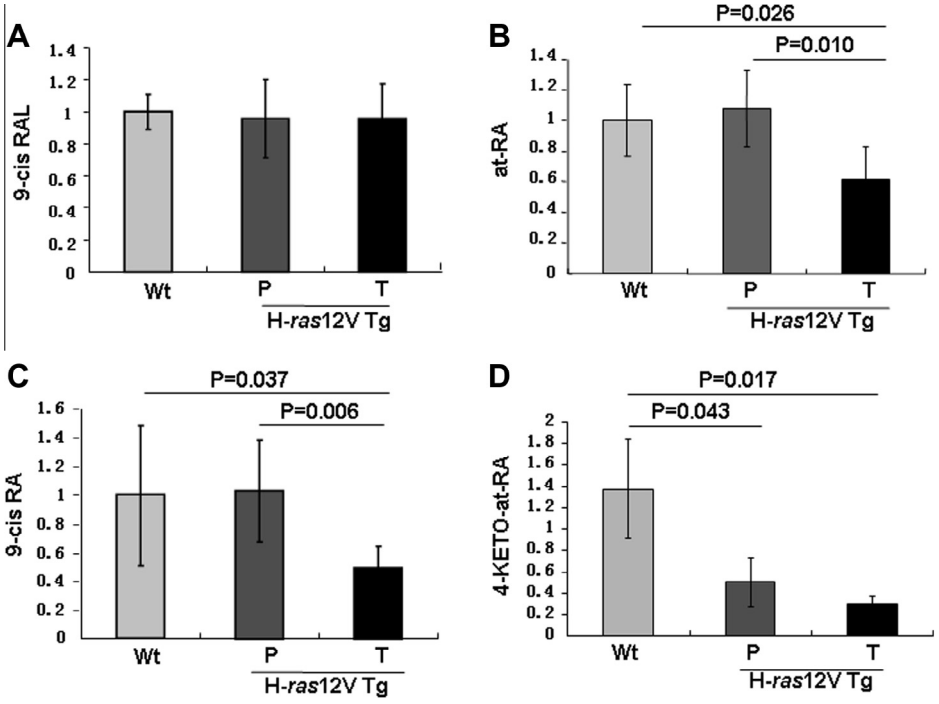

Fig. 2. Quantitative analysis of retinoid metabolites in samples by high performance liquid chromatography. (A) 9-cis RAL. (B) at-RA. (C) 9-cis RA. (D) 4-KETO-at-RA. The Wt, P, and T refer to the same as Fig. 1. Data are expressed as mean ± S.D. ($n = 6$).

in vivo data showed that, like CYP genes, the expressions of ALDH1A1 and AOX3 were also directly repressed by *ras* oncogene (Fig. 1). Moreover, down-regulation of the ALDH1A1, AOX3, and CYP genes induced by *ras* oncogene may favor the metabolism state and the progress of hepatoma by disturbing multiple metabolism processes.

AtRA has been used as a main drug component to treat acute promyelocytic leukemia (APL) patients in clinical [21]. It is also reported epidemiologically and experimentally that atRA could prevent cancer in various organs including the liver, stomach, breast, lung, and prostate [10]. There is an *in vivo* inter-conversions between atRA and 9cRA isomers, two active forms of RA known to activate retinoid receptors, especially the heterodimer RXR:RAR [22,23]. So, it is generally thought that atRA exerts its antitumor effects through activation of RXR:RAR. On the contrary, our results showed no effect of atRA on preventing hepatic tumorigenesis or curing the developed hepatic nodules induced by *ras* oncogene (Fig. 4). Consistently, multiple resistance mechanisms to atRA application have been reported in organisms and cells [24]. Specially, it is well known that HCC is refractory to RA due to malfunction of its nuclear receptor RXRα [25]. The progressive resistance to continuous atRA treatment [26] and the loss of function of RXRα [25] may be the two main reasons contributing to our experimental results.

In conclusion, activated RAS/ERK pathway alone is insufficient to inhibit the functions of RXRα and deplete RA in normal hepatocytes. The efficient inhibition of RXRα function and depletion of RA in hepatoma indicates that additional molecular events must be involved besides activation of RAS/ERK pathway.

Conflict of interest

The authors have nothing to declare.

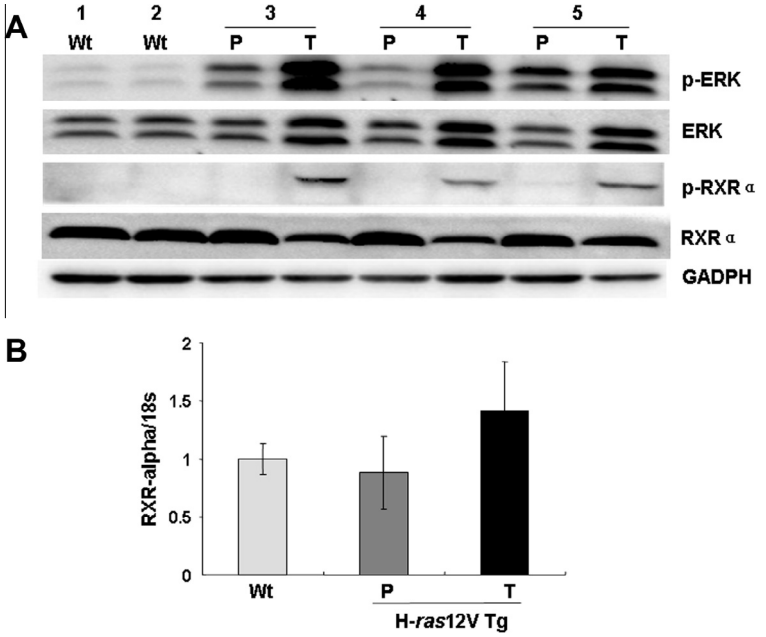

Fig. 3. Activation of RAS/ERK signaling pathway blocks the functions of RXRα in hepatic tumor. (A) The protein levels of p-ERK, ERK, p-RXRα and RXRα were detected by western blot. GAPDH was used as loading control. The numbers 1–5 indicates individual mouse. (B) The mRNA expression level of RXRα were detected by RT-qPCR and normalized to 18s. The Wt, P, and T refer to the same as Fig. 1. Data are expressed as mean ± S.D. (n = 5).

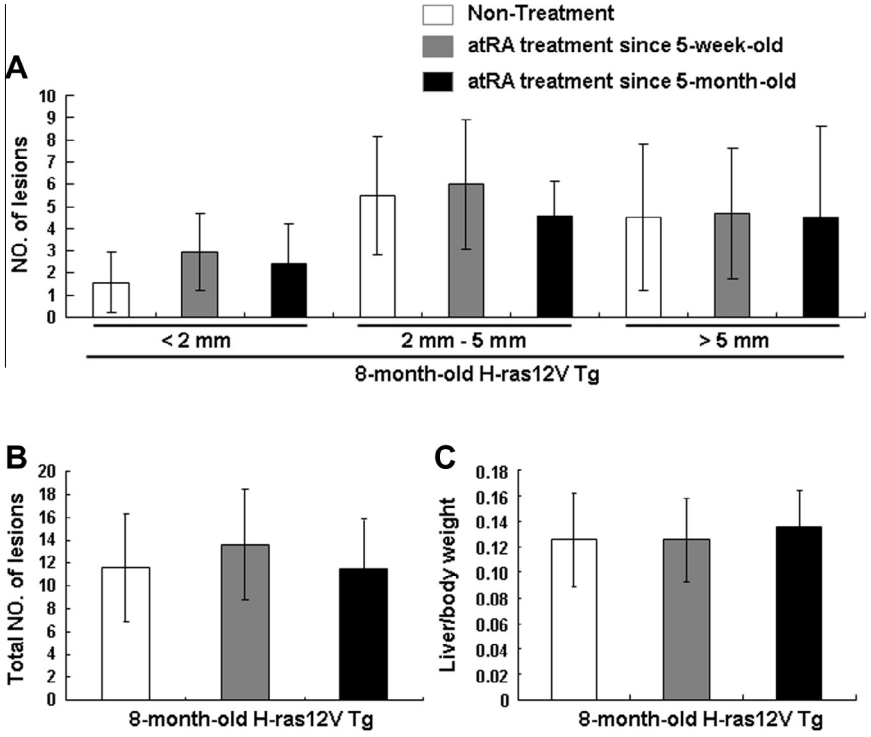

Fig. 4. No effect of atRA on preventing hepatic tumorigenesis and curing the developed hepatic nodules induced by *ras* oncogene. H-*ras*12V transgenic mice were applied with atRA in daily food (8.33 mg/kg/day) started at 5-week-old (no hepatic lesions) and 5-month-old (multiple nodules in liver), respectively. H-*ras*12V transgenic mice feed with normal food as control. The mice were sampled at 8-month-old and the number of hepatic lesions according to diameter (<2 mm; 2–5 mm; >5 mm) (A), the total number of hepatic lesions (B), and the liver/body weight (C) were analyzed. Data are expressed as mean ± S.D. (n = 10–15).

Acknowledgment

This research was supported by grants from the National Natural Science Foundation of China (General Program, No. 30872950).

Appendix A. Supplementary data

Supplementary data associated with this article can be found, in the online version, at http://dx.doi.org/10.1016/j.bbrc.2014.09.007.

References

[1] J.D. Yang, L.R. Roberts, Hepatocellular carcinoma: a global view, Nat. Rev. Gastroenterol. Hepatol. 7 (2010) 448–458.
[2] S.F. Altekruse, K.A. McGlynn, M.E. Reichman, Hepatocellular carcinoma incidence, mortality, and survival trends in the United States from 1975 to 2005, J. Clin. Oncol. 27 (2009) 1485–1491.
[3] H.K. Seitz, F. Stickel, Risk factors and mechanisms of hepatocarcinogenesis with special emphasis on alcohol and oxidative stress, Biol. Chem. 387 (2006) 349–360.
[4] H.B. El-Serag, H. Hampel, F. Javadi, The association between diabetes and hepatocellular carcinoma: a systematic review of epidemiologic evidence, Clin. Gastroenterol. Hepatol. 4 (2006) 369–380.
[5] V. Paradis, S. Zalinski, E. Chelbi, N. Guedj, F. Degos, V. Vilgrain, P. Bedossa, J. Belghiti, Hepatocellular carcinomas in patients with metabolic syndrome often develop without significant liver fibrosis: a pathological analysis, Hepatology 49 (2009) 851–859.
[6] G. Baffy, E.M. Brunt, S.H. Caldwell, Hepatocellular carcinoma in non-alcoholic fatty liver disease: an emerging menace, J. Hepatol. 56 (2012) 1384–1391.
[7] Y. Midorikawa, Y. Sugiyama, H. Aburatani, Molecular targets for liver cancer therapy: from screening of target genes to clinical trials, Hepatol. Res. 40 (2010) 49–60.
[8] P. Newell, S. Toffanin, A. Villanueva, D.Y. Chiang, B. Minguez, L. Cabellos, R. Savic, Y. Hoshida, K.H. Lim, P. Melgar-Lesmes, S. Yea, J. Peix, K. Deniz, M.I. Fiel, S. Thung, C. Alsinet, V. Tovar, V. Mazzaferro, J. Bruix, S. Roayaie, M. Schwartz, S.L. Friedman, J.M. Llovet, Ras pathway activation in hepatocellular carcinoma and anti-tumoral effect of combined sorafenib and rapamycin in vivo, J. Hepatol. 51 (2009) 725–733.
[9] Y. Muto, H. Moriwaki, Antitumor activity of vitamin A and its derivatives, J. Natl. Cancer Inst. 73 (1984) 1389–1393.
[10] K. Kanki, Y. Akechi, C. Ueda, H. Tsuchiya, H. Shimizu, N. Ishijima, K. Toriguchi, E. Hatano, K. Endo, Y. Hirooka, G. Shiota, Biological and clinical implications of retinoic acid-responsive genes in human hepatocellular carcinoma cells, J. Hepatol. 59 (2013) 1037–1044.
[11] M. Shimizu, Y. Shirakami, K. Imai, K. Takai, H. Moriwaki, Acyclic retinoid in chemoprevention of hepatocellular carcinoma: targeting phosphorylated retinoid X receptor-alpha for prevention of liver carcinogenesis, J. Carcinog. 11 (2012) 11.
[12] M. Shimizu, K. Imai, K. Takai, H. Moriwaki, Role of acyclic retinoid in the chemoprevention of hepatocellular carcinoma: basic aspects, clinical applications, and future prospects, Curr. Cancer Drug Targets 12 (2012) 1119–1128.
[13] C. Fremin, F. Ezan, J.P. Guegan, L. Gailhouste, M. Trotard, J. Le Seyec, J. Rageul, N. Theret, S. Langouet, G. Baffet, The complexity of ERK1 and ERK2 MAPKs in multiple hepatocyte fate responses, J. Cell. Physiol. 227 (2012) 59–69.
[14] A. Braeuning, Regulation of cytochrome P450 expression by Ras- and beta-catenin-dependent signaling, Curr. Drug Metab. 10 (2009) 138–158.
[15] H. Shiraha, K. Yamamoto, M. Namba, Human hepatocyte carcinogenesis (review), Int. J. Oncol. 42 (2013) 1133–1138.
[16] A.G. Wang, H.B. Moon, M.R. Lee, C.Y. Hwang, K.S. Kwon, S.L. Yu, Y.S. Kim, M. Kim, J.M. Kim, S.K. Kim, T.H. Lee, E.Y. Moon, D.S. Lee, D.Y. Yu, Gender-dependent hepatic alterations in H-ras12V transgenic mice, J. Hepatol. 43 (2005) 836–844.
[17] A. Baba, M. Shimizu, T. Ohno, Y. Shirakami, M. Kubota, T. Kochi, D. Terakura, H. Tsurumi, H. Moriwaki, Synergistic growth inhibition by acyclic retinoid and phosphatidylinositol 3-kinase inhibitor in human hepatoma cells, BMC Cancer 13 (2013) 465.
[18] T. Smutny, M. Bitman, M. Urban, M. Dubecka, R. Vrzal, Z. Dvorak, P. Pavek, U0126, a mitogen-activated protein kinase kinase 1 and 2 (MEK1 and 2) inhibitor, selectively up-regulates main isoforms of CYP3A subfamily via a pregnane X receptor (PXR) in HepG2 cells, Arch. Toxicol. (2014).
[19] H. Chen, Z.Y. Shen, W. Xu, T.Y. Fan, J. Li, Y.F. Lu, M.L. Cheng, J. Liu, Expression of P450 and nuclear receptors in normal and end-stage Chinese livers, World J. Gastroenterol. 20 (2014) 8681–8690.
[20] A. Braeuning, M. Schwarz, Zonation of heme synthesis enzymes in mouse liver and their regulation by beta-catenin and Ha-ras, Biol. Chem. 391 (2010) 1305–1313.
[21] F. Lo-Coco, S.K. Hasan, Understanding the molecular pathogenesis of acute promyelocytic leukemia, Best Pract. Res. Clin. Haematol. 27 (2014) 3–9.
[22] M. Le Vee, E. Jouan, B. Stieger, O. Fardel, Differential regulation of drug transporter expression by all-trans retinoic acid in hepatoma HepaRG cells and human hepatocytes, Eur. J. Pharm. Sci. 48 (2013) 767–774.
[23] H. Chen, M.R. Juchau, Biotransformation of 13-cis- and 9-cis-retinoic acid to all-trans-retinoic acid in rat conceptual homogenates. Evidence for catalysis by a conceptual isomerase, Drug Metab. Dispos. 26 (1998) 222–228.
[24] M. Li, Y. Sun, X. Guan, X. Shu, C. Li, Advanced progress on the relationship between RA and its receptors and malignant tumors, Crit. Rev. Oncol. Hematol. (2014).
[25] R. Matsushima-Nishiwaki, M. Okuno, Y. Takano, S. Kojima, S.L. Friedman, H. Moriwaki, Molecular mechanism for growth suppression of human hepatocellular carcinoma cells by acyclic retinoid, Carcinogenesis 24 (2003) 1353–1359.
[26] N. Idres, J. Marill, G.G. Chabot, Regulation of CYP26A1 expression by selective RAR and RXR agonists in human NB4 promyelocytic leukemia cells, Biochem. Pharmacol. 69 (2005) 1595–1601.